JOURNAL OF APPLIED ELECTROCHEMISTRY 23 (1993) 863–872

Maskless zinc electrodeposition assisted by a pulsed laser beam

I. ZOUARI, C. PIERRE, F. LAPICQUE

Laboratoire des Sciences du Génie Chimique, CNRS-ENSIC-INPL, BP 451, F-54001 Nancy, France

M. CALVO

Laboratoire de Science et Génie des Matériaux Métalliques, URA CNRS 159, Ecole des Mines, F-54042 Nancy, France

Received 11 July 1992; revised 4 December 1992

This paper deals with jet electrodeposition for the production of maskless deposits and patterns of a well-defined shape, and the potential improvements allowed by a pulsed laser beam. On the basis of the example of zinc deposition in a sulphate medium, several aspects of this type of deposition (mass transfer rate, i–E curves, morphology of the deposit, and the effect of a pulsed YAG laser beam at 532 nm) are presented. Laser assistance has no significant effect on the deposition current. Pulsed irradiation improves zinc morphology by an appreciable grain coalescence and a reduction in grain size; this results in increased precision of the maskless deposits, the central zones of which are as wide as the nozzle.

Nomenclature

D diffusion coefficient ($m^2 s^{-1}$)
d nozzle diameter (m)
E electrode potential (V)
F Faraday constant (96 487 A s mol^{-1})
I current (A)
I_L limiting current (A)
i current density ($A m^{-2}$)
i_L limiting current density ($A m^{-2}$)
k_d mass transfer coefficient ($m s^{-1}$)
l distance between nozzle and cathode (m)
M molecular weight of deposited metal ($kg mol^{-1}$)
Re Reynolds number $= ud/\nu$
r deposition rate ($m s^{-1}$ or $\mu m s^{-1}$)
r_L deposition rate under diffusional control ($m s^{-1}$ or $\mu m s^{-1}$)
Sc Schmidt number $= \nu/D$
Sh Sherwood number $= k_d d/D$
u average velocity of the liquid in the jet ($m s^{-1}$)
x Axial coordinate in the jet (m)

Greek symbols
κ Electrical conductivity ($\Omega^{-1} m^{-1}$)
ν Kinematic viscosity ($m^2 s^{-1}$)
ν_e number of electrons
ρ density of metal deposited ($kg m^{-3}$)

1. Introduction

Impinging jets at electrode surfaces have been used for decades in numerous applications, for example, electrochemical analysis [1] and the study of particular electrode reactions such as EC or ECE processes [2, 3]. However, the most common use is high-speed electrochemical deposition or etching [4, 5]. The high mass transfer rates at the electrode allow substantial reduction in processing time for the manufacture of specified pieces for the electronics industry: typical processing rates are of several micrometres per second. In addition, jet devices offer the following advantages: possible maskless operation, recycle of expensive electrolyte solution, use of dilute solutions, and possible manufacture of metal circuits of controlled geometry. Jet plating technology involves precious metals but also copper, tin, zinc or alloys. The metal deposited with a jet device can be of higher quality, e.g. structure or ductility, than metal layers electroplated in classical devices [5].

Some years ago, von Gutfeld and co-workers suggested the use of a laser beam to improve the performance of jet plating. Laser assistance can increase deposition rate by reducing the importance of side reactions, as for example with gold under the beam of a continuous wave argon laser [6, 7]. Also, the use of a continuous laser is reported to improve the metal quality, for example, morphology, compactness, and electrical conductivity as a consequence.

Laser assistance has also been used in other electrochemical systems, such as RDE or flat parallel electrodes, for various metals [8–11]. Irradiation by continuous laser beam has been reported to induce microstirring phenomena near the irradiated surface and to increase charge transfer phenomena [8]. More recently, the assistance of a pulsed laser beam was investigated for the example of zinc deposited in a flat parallel electrode reactor. Zinc deposition from

0021-891X

a sulphate medium was selected since it is a troublesome deposition reaction when carried out in the absence of additive substance. The sharp increase of temperature at the metal surface during each energy pulse was shown to improve the deposition with regard to the available current density and the deposit morphology. Indeed pulsed laser irradiation hinders the formation of dendrites, allows a reduction in the size of metal grains, and results in coalesced deposits [11, 12]. In addition, the reduction current was observed to be increased by the laser beam power, depending on hydrodynamic conditions [11].

The present study deals with the jet-plating electrodeposition of zinc in a sodium sulphate medium and the effect of a pulsed YAG laser beam on the performance of this deposition. After a short characterization of the device used in terms of mass transfer rate, the paper describes the influence on the deposition of various operating parameters, namely zinc concentration, current density (or electrode potential) and power of the pulsed laser beam. Zinc electrodeposition was examined with respect to current density and metal morphology.

2. Experimental details

2.1. Chemical system

The electrodeposition of zinc in a jet-plating device was investigated for a zinc sulphate solution: the concentration of the introduced zinc was varied from 0.01 up to 0.7 M. Sodium sulphate kept at 0.2 M, acted as a supporting electrolyte. Both sulphate salts were of analytical grade (Prolabo, France). Physicochemical data of the solutions were measured: values of pH, viscosity and electrical conductivity are reported in Table 1, depending on the concentration of zinc sulphate.

Diffusion coefficient of zinc species was estimated by linear voltammetry using a rotating disc electrode [13] and was shown to be near $5.0 \times 10^{-10}\,m^2\,s^{-1}$ at 25 °C in the range 0.01–0.15 M. This value has been assumed to hold for more concentrated solutions.

2.2. Setup

The experimental setup is schematically shown in Fig. 1. A glass tank provided with water jacket acts as a solution reservoir and the temperature was maintained at 25 ± 0.5 °C for all experiments. The

Table 1. Physicochemical properties of the 0.2 M Na_2SO_4 solutions used

$[ZnSO_4]$/mol dm^{-3}	*0.01*	*0.07*	*0.70*
pH	5.68	5.07	4.02
$\nu/10^{-6}\,m^2\,s^{-1}$	0.96	0.98	1.28
$\kappa/\Omega^{-1}\,m^{-1}$	2.98	3.10	5.00

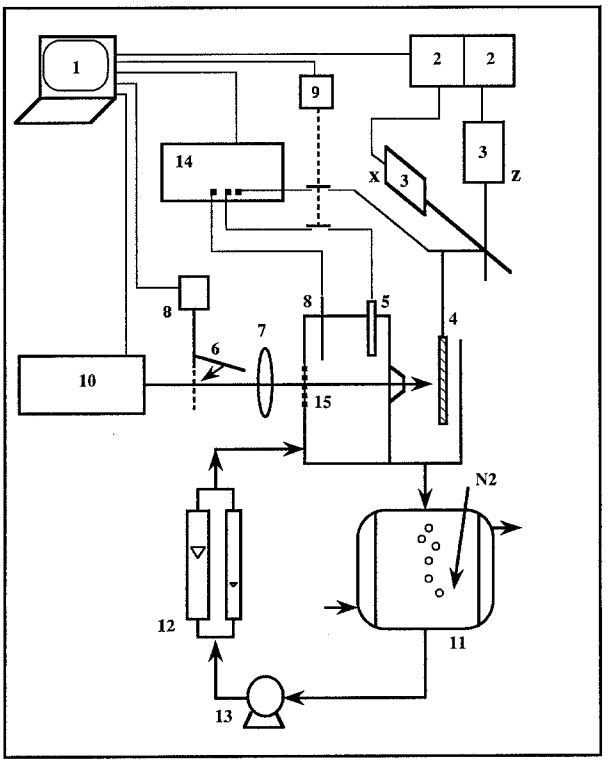

Fig. 1. Schematic representation of the experimental setup: (1) Computer, (2) interface boards, (3) step-by-step motor, (4) working electrode, (5) reference electrode, (6) counter electrode, (7) convergent lens, (8) chopper, (9) electric relay, 10: YAG (532 nm) pulsed laser, (11) reservoir, (12) flow meters, (13) gear pump, (14) potentiostat, and (15) quartz window.

solution was degasified with nitrogen prior to deposition trials. The liquid was driven by a gear pump into the jet device at a chosen flow rate. The cell design was derived from that proposed by von Gutfeld. The cell was machined out of methyl polymethacrylate; it consisted of an inlet chamber, the nozzle, and the substrate support facing the nozzle section. The nozzle was a conical piece drilled with a hole of well-defined diameter, which is of major importance for hydrodynamics of the jet; three nozzles were used, their orifice diameter being 0.30, 0.50 or 1.00 mm. A reference electrode (SCE) and a platinum sheet anode were placed in the inlet chamber. The cathode was a 0.5 mm thick zinc foil attached to a microcomputer-controlled X–Z table via an extension arm: the substrate was displaced in a plane perpendicular to the horizontal liquid jet.

A YAG pulsed laser was used at 532 nm. The repetition rate was kept to 30 Hz and the energy was delivered in a time span of 8×10^{-9} s. The laser beam entered the quartz window and emerged colinearly to the jet through the nozzle. The average incident power was limited to 2 W to avoid bubble formation on the substrate.

The deposition was carried out under controlled potential using a PAR 362 potentiostat and the cell current was continuously recorded. The computer used (Olivetti M 250) was equipped with an interface board: this device was programmed to ensure the motion of the cathode, to synchronize the gate-on of the laser beam with the closure of the electrical circuit, and to collect the experimental data.

3. Hydrodynamics of the jet and mass transfer

Before describing the effect of the laser beam on jet deposition of zinc, this part is devoted to the hydrodynamic conditions used for the deposition trials. Additionally, mass transfer rates at the facing electrode can yield maximal estimates for current density, to be compared to the operating current densities for zinc deposition.

3.1. Hydrodynamics

The hydrodynamics of unsubmerged jets has been well described [14]. Velocity profile and hydrodynamics depend on the relative axial abscissae, x/d, where d is the nozzle diameter. The first zone, for x/d less than 6.2, is the development region; there, an internal core with flat velocity profile is surrounded by a boundary layer. The second part of the jet, for which x/d is in the range 6.2–8, is a transition zone and is generally neglected. The velocity profile is established in the third part ($8 < x/d < 100$) but the conical shape of the jet results in a decrease in the average velocity.

The distance between the nozzle outlet and the substrate, 1, was fixed at $6.2x$ for all cases. Therefore, velocity profile can be considered as established and the diameter of the jet can be approximated to that of the nozzle used. However, the presence of a solid facing the jet likely affects its hydrodynamics: when hitting the surface, the fluid spreads out as a thin liquid film and flows radially outwards from the point of impingement.

Reynolds numbers over 2000 are required for turbulent flow. With a kinematic viscosity of $10^{-6}\,m^2\,s^{-1}$, this constraint requires an average velocity above $2\,m\,s^{-1}$ for a 1 mm diameter nozzle; the minimal velocity should be $6\,m\,s^{-1}$ for the smallest nozzle considered. However, the velocity of the liquid flowing in the smallest nozzle cannot exceed $15\,m\,s^{-1}$ to obtain a continuous jet. As a matter of fact, when the pressure upstream of the nozzle exceeds a certain limit, the sharp pressure drop is accompanied by spray formation. This phenomenon limits the use of free jets through a very small nozzle. For the reasons given above, the average velocity was varied from 2 to $15\,m\,s^{-1}$.

3.2. Mass transfer

Heat and mass transfer at solid surfaces facing impinging jets has been extensively investigated. Most theoretical contributions deal with submerged jets because of the continuity of the boundary conditions involved. Nevertheless, the case of unsubmerged jets has been examined by several authors [15, 16]. In fact, two mass transfer phenomena have to be examined: in the impinging zone (i), and in the surrounding zone (ii). For the present purpose of maskless patterning, only transfer in the impinging zone was considered. The jet is usually vertical, the liquid flowing upwards [15] or downwards [16]. The dimensionless correlation, established by Chin and Tsang [17] for submerged turbulent jets, provides the representative mass transfer rate for Re number greater than 3000 for both submerged and unsubmerged jets:

$$Sh = 0.86 Re^{1/2} Sc^{1/3} g(Sc) \qquad (1)$$

where the function $g(Sc)$ can be approximated to $1-0.0846 Sc^{-1/3}$ for most liquids.

In contrast to the arrangement considered in [15–17], the jet plating device relies upon a horizontal jet of liquid. For this reason, mass transfer rates were determined by measurement of limiting current of the electrochemical reduction of potassium ferricyanide in a 0.5 M NaOH medium, and the zinc substrate was replaced by a nickel foil. The cathode was activated prior to each measurement by hydrogen evolution for 10 min. The distance between the foil and the largest nozzle (diam. 1 mm) was fixed at 6.2 mm. In spite of the distribution of turbulence level near the impinged surface, current density and mass transfer coefficient were calculated as the ratio of the measured current over the cross section of the jet. The current recorded as a function of the average velocity in the range $2–10\,m\,s^{-1}$, yielded the following relation:

$$Sh = 6.7 Re^{1/2} Sc^{1/3} \qquad (2)$$

The large discrepancy between Equations 1 and 2 may stem from the direction of the liquid jet. Correlation 2 corresponds to mass transfer coefficient over $10^{-3}\,m\,s^{-1}$ in the considered velocity range, which may seem large when compared to the values reported in [16]. However, jet deposition of copper in a comparable cell was shown to occur at a very high current density with current efficiency near unity [6]. The highest current density reported provided a minimal estimate for k_d near $8 \times 10^{-3}\,m\,s^{-1}$ in the case of a 1 M $CuSO_4$ solution flowing at $10\,m\,s^{-1}$ out of a 0.5 mm nozzle. Applying Equation 2 to zinc deposition at 25 °C under similar hydrodynamics leads to a mass transfer coefficient of $6.0 \times 10^{-3}\,m\,s^{-1}$, which is consistent with the value estimated from published data.

Correlation 2 allows the limiting current density of zinc deposition to be predicted as a function of fluid velocity, nozzle diameter and zinc sulphate concentration. In addition, assuming 100% current efficiency for zinc jet deposition leads to the relationship between deposition rate, r, and current density:

$$r = \frac{iM}{\nu_e F \rho} \qquad (3)$$

Table 2. Theoretical values for current density and deposition rate under diffusional control

$[ZnSO_4]$/mol dm^{-3}	*0.01*	*0.07*	*0.70*
i_L/A m^{-2}	1.11×10^4	7.74×10^4	7.38×10^5
r_L/μm s^{-1}	0.527	3.67	35.0

where M denotes the molecular weight of zinc, ν_e the number of electrons involved in the deposition, and ρ the density. For the present case of zinc deposition, the ratio (r/i) equals $4.745 \times 10^{-11}\,m\,s^{-1}\,A^{-1}\,m^2$. Table 2 reports values of both the current density and the deposition rate under diffusional control, depending on the concentration of zinc sulphate. The thickness of the deposit was estimated from the current density and Relation 3, taking into account the deposition time or the displacement speed of the substrate.

4. General aspects of zinc jet electrodeposition

Before describing the effect of the laser beam and the influence of significant parameters on the morphology of deposited metal, general trends of the deposition performed without laser assistance are first presented, namely the available current density for the deposition and the morphology of the deposits.

4.1. i–E curves: importance of ohmic drop

Linear voltammetry experiments were conducted in order to measure the limiting current and to obtain the potential domain for zinc deposition with no hydrogen evolution. The scan rate was fixed at $5\,mV\,s^{-1}$. Current density increased linearly with potential in the range -1.1 and -5 V vs SCE, as shown in Fig. 2; no diffusional plateau could be observed, even for potentials as far as -10 V, due to the significance of ohmic drop in the cell, especially in the liquid jet. The resistance of the liquid jet was estimated by measurements of the potential difference and the current between the cathode and the reference electrode; this resistance was also calculated on the basis of the cylinder of liquid, in good agreement with experimental data. The resistance of the liquid jet usually exceeded $2000\,\Omega$ and, in spite of a weak deposition current, the ohmic drop could attain 30 V.

4.2. Shape of the deposits

Most deposits consisted of lines: the length of the line was limited to 10 mm and the substrate velocity was fixed at $67\,\mu m\,s^{-1}$. For low current densities, the deposits were of thickness far below $1\,\mu m$: for these cases, successive scans were carried out on the same area and yielded thicker deposits.

The liquid jet created a thin layer around the impingement point and flowed down the cathode surface due to gravity. Therefore, the direction of the cathode displacement was expected to influence the deposition. When the substrate descended vertically, the liquid jet hit a clean cathode surface; in the case of vertical upwards displacement, the surface was covered with a thin existing layer. Line depositions conducted in the potentiostatic mode revealed that the direction of the substrate in vertical displacement affected the recorded current: the current increased slightly with time when lifting the zinc substrate; it decreased when descending. The current was constant for horizontal patterning.

The shape of the zinc deposits was satisfactory with respect to its width and the regularity of the metal. Figure 3 shows that zinc was deposited on two zones: (i) a central zone, A, corresponding to the deposit itself, and (ii) a larger zone, B, surrounding the central zone. The width of zone A was equal to the nozzle diameter within 5%. The existence of part B is probably due to liquid spreading on the metal surface around the impingement point and subsequent

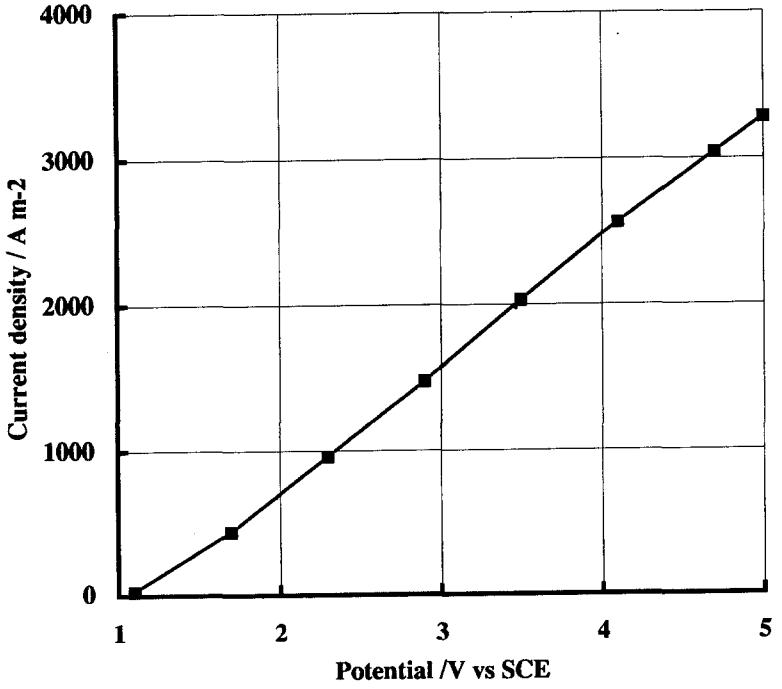

Fig. 2. Example of i–E variation for zinc electrodeposition from a 0.07 M $ZnSO_4$, 0.2 M Na_2SO_4 solution; nozzle diameter: 1 mm.

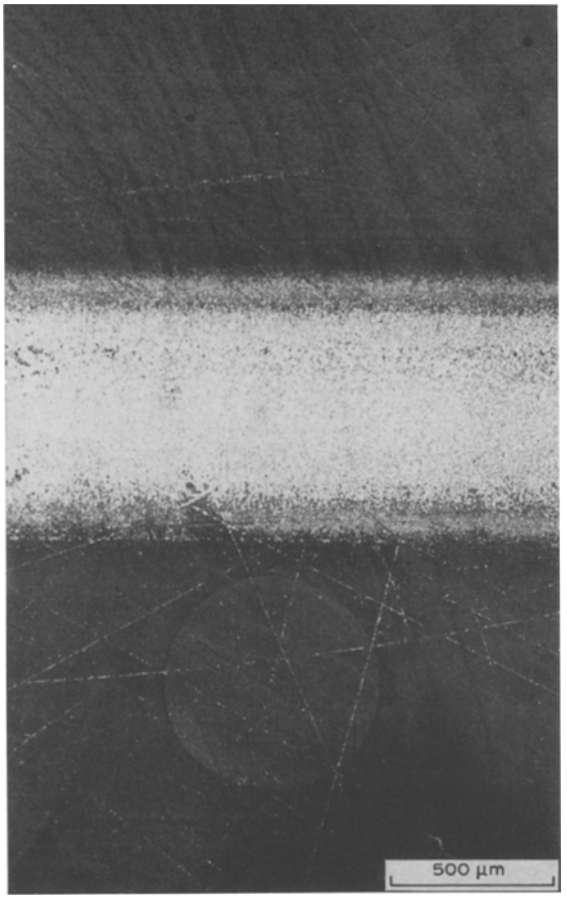

Fig. 3. View of a zinc deposit produced in the absence of laser beam in the following conditions: $[ZnSO_4] = 0.01$ M; $E = -1.5$ V vs SCE, i.e. $i = 440\,A\,m^{-2}$; nozzle diam: 0.5 mm; fluid velocity: $9.1\,m\,s^{-1}$; deposit thickness: 0.8 μm.

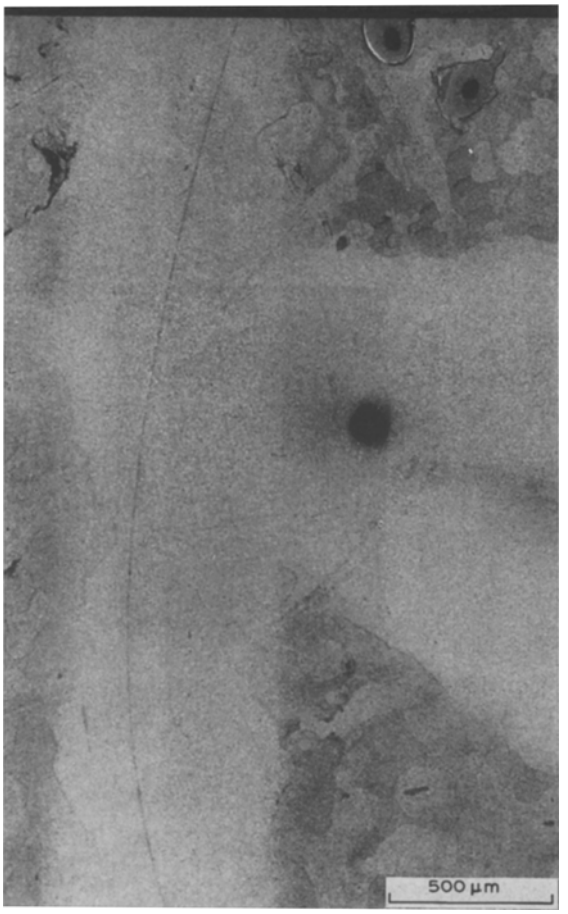

Fig. 4. Example of zinc patterning: part view of the letter 'R' written on the zinc substrate; $[ZnSO_4] = 0.7$ M; $E = -3.0$ V vs SCE, i.e. $i = 3060\,A\,m^{-2}$; nozzle diameter: 0.5 mm; fluid velocity: $9.1\,m\,s^{-1}$; deposit thickness: 1.1 μm.

side-deposition of metal in this zone. SEM observations showed that the deposit in part B was very thin compared to that of zone A, which justified the calculation of current density on the basis of the jet cross section.

Deposits of other pattern were also produced using the computer-controlled X–Z table. Figure 4 shows that the shape of the deposit was well-defined, especially near the change of direction of the substrate displacement. As observed for the line patterning, the deposit core was surrounded by a very thin peripheral zone.

4.3. Morphology of zinc deposit

Typically, zinc deposits consisted of two types of layers. The first layer consisted of small grains formed in the nucleation step; this layer was covered by a layer of different structure, consisting of larger grains.

Jet velocities up to 15 or $20\,m\,s^{-1}$ result in irregular deposit for which the external layer did not entirely cover the inner layer. This may be due to the poor adherence of zinc and the high kinetic energy of the jet: zinc crystals present on previously deposited metal, were washed off by the impinging jet. The average velocity of the liquid was thereafter limited to $10\,m\,s^{-1}$. In addition, most deposits were produced with a 0.5 mm nozzle.

Figure 5(a) and (b) presents SEM views of a deposit obtained at -1.5 V vs SCE from a 0.01 M $ZnSO_4$ solution, with one and five scans. The average thickness of one layer was estimated to 0.16 μm from the current recorded and using Equation 3. The compactness of the deposit increased from the first to the last layer. The deposit consisted of fine needles, which indicated a predominant control by electrode kinetics. Figure 5 shows that successive scans allowed deposit growth through increase in the number of grains, the grain size remaining unchanged.

As expected, the electrode potential exerted a strong influence on zinc morphology. A more compact morphology was produced at higher overvoltage. Deposits produced under partial diffusion control exhibited well-defined grains with no connection to each other. For such conditions, successive scans resulted in growth of the grains in the existing layers which resulted in a more homogeneous deposit.

5. Effect of a pulsed laser beam on jet deposition

5.1. Deposition current

For all conditions investigated, laser assistance was shown to have a weak influence on the current

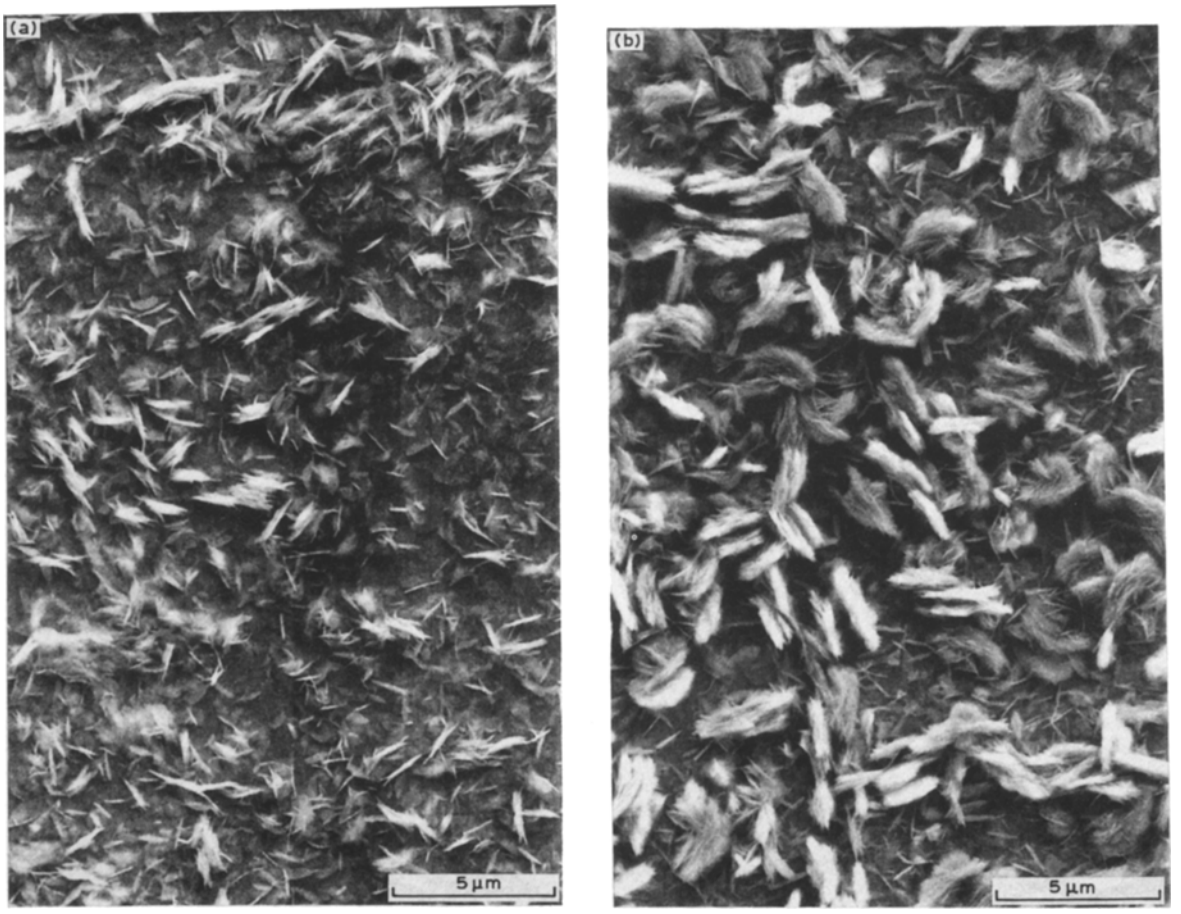

Fig. 5. Successive layers of a deposit obtained in the following conditions: $[ZnSO_4] = 0.01$ M; $E = -1.5$ V vs SCE (i/i_L near 0.04); nozzle diameter: 0.5 mm; fluid velocity: 9.1 m s^{-1}; thickness of one layer: 0.16 μm. (a) One layer and (b) five layers.

for a given potential. Figure 6 gives a representative example. This low effect was explained as follows:

(i) The shape of the i–E curves was largely affected by the significant ohmic drop and an eventual effect of laser beam on the current density was therefore masked by this voltage contribution;
(ii) Microstirring phenomena near the solid-liquid interface mentioned in [8] cannot be generated to a sufficient extent within the pulse duration, due to the slowness of both mass and momentum transfer. The pulsed laser beam may only modify phenomena occurring at the electrode surface e.g. electron transfer or crystallization.
(iii) The strong turbulence of the electrolyte solution near the electrode may enlarge the heat loss during the relaxation period and accelerate the temperature decrease at the interface: this cooling effect may

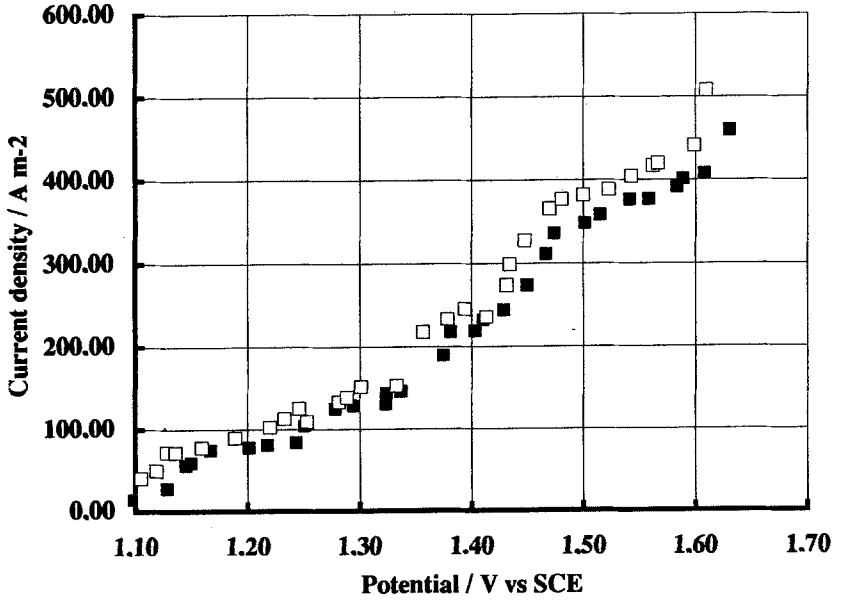

Fig. 6. Example of i–E variation for zinc deposition with laser assistance (□) and without (■); $[ZnSO_4] = 0.07$ M; nozzle diam.: 1 mm.

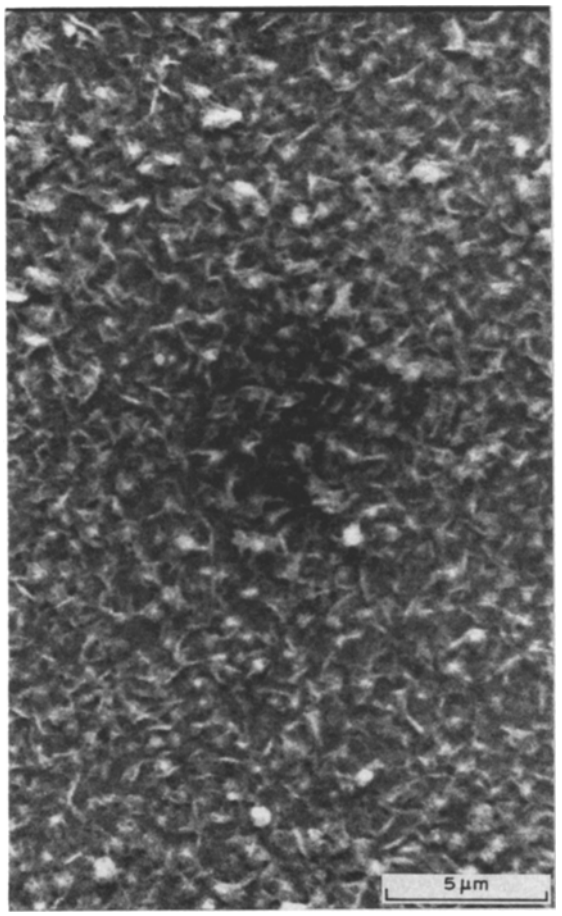

Fig. 7. Deposit obtained in the following conditions: $[ZnSO_4] = 0.01$ M; i/i_L near 0.04; nozzle diameter: 0.5 mm; fluid velocity: 9.1 m s^{-1}; laser power: 2 W; deposit thickness: 0.16 μm.

reduce both the duration of interface heating and the laser efficiency.

5.2. *Morphology of the deposit*

Laser deposition did not change the general appearance of the deposit. The light beam was guided by the liquid jet to the zinc substrate and the effect of the laser was therefore located on to the central part (A) of the deposit. Observation of part B of deposits, produced with or without laser, revealed no significant difference in the morphology. The effect of the laser beam on the morphology of part A was investigated for various conditions of current density, zinc concentration and electrode potential.

Reduced current density (i/i_L) was considered as an operating parameter to quantify the significance of diffusion control in the deposition process. The high ohmic drop in the jet led to the use of low concentrations of zinc sulphate to this purpose. Figures 5(a) and 7 refer to zinc deposition from a 0.01 M $ZnSO_4$ solution and a ratio i/i_L near 0.04: the deposits obtained consisted of needles, corresponding to kinetic control. However, more regular deposit of smaller needles were obtained with laser assistance (Fig. 7), as compared to the deposit of Fig. 5(a). For higher values of reduced current density, the morphology was improved with respect to its regularity and compactness (Fig. 8). For a current density of the order of i_L, the 'cauliflower' appearance of the deposit obtained in the absence of the laser was changed to grains of more uniform size. In addition, the needles making up the grains were of smaller dimensions and the grain became flake-like in appearance (Fig. 9). Coalescence phenomena observed with a parallel electrode cell were also generated by the pulsed laser beam for jet plating operations.

Similar observations can be made for higher concentrations such as 0.07 M, under either kinetic or mixed control. Figure 10 presents deposits obtained under kinetic control, for i/i_L near 0.03. The laser beam resulted in smaller needles forming the grains but the grain dimension was not significantly affected. For higher current densities, the structure of the grain was affected by laser irradiation, as shown in Fig. 11: whereas each grain produced with classical conditions was formed with parallel needles, the mean direction of these needles cannot be defined with laser assistance, due to their very small size. Increasing the zinc sulphate concentration may improve the deposit morphology. The deposit obtained without the laser from a 0.7 M solution in the kinetic regime (Fig. 12a) is fairly regular; laser assistance results in a smoothing of the surface but some irregular grains can be observed, as shown in Fig. 12(b).

6. Conclusion

Zinc deposition from a sulphate medium can be achieved in jet plating devices for the production of maskless deposits. Care should be taken when performing such deposition to ensure satisfactory adherence of the metal on the substrate. As demonstrated earlier for other metal depositions, the pattern deposition of zinc can be carried out using a jet device: the width of the central area corresponds to the nozzle diameter, in the range 0.3–1 mm, and the side-deposit in the surrounding zone could be removed by subsequent dissolution.

The effect of laser assistance on both current density and deposit morphology was weaker for jet plating devices as compared to other devices such as parallel plate electrode cells: current density at the surface of the impinged electrode was not significantly enhanced. With respect to morphology, use of a pulsed laser allows a reduction in the size of the needles forming the grains and slight coalescence phenomena was observed: these phenomena result in higher compactness of the central part of the deposit. The main reasons for the moderate effect of the laser irradiation have been discussed above. In addition, high deposition rates are allowed by jet devices and the amount of material deposited between each energy pulse is far higher than that in

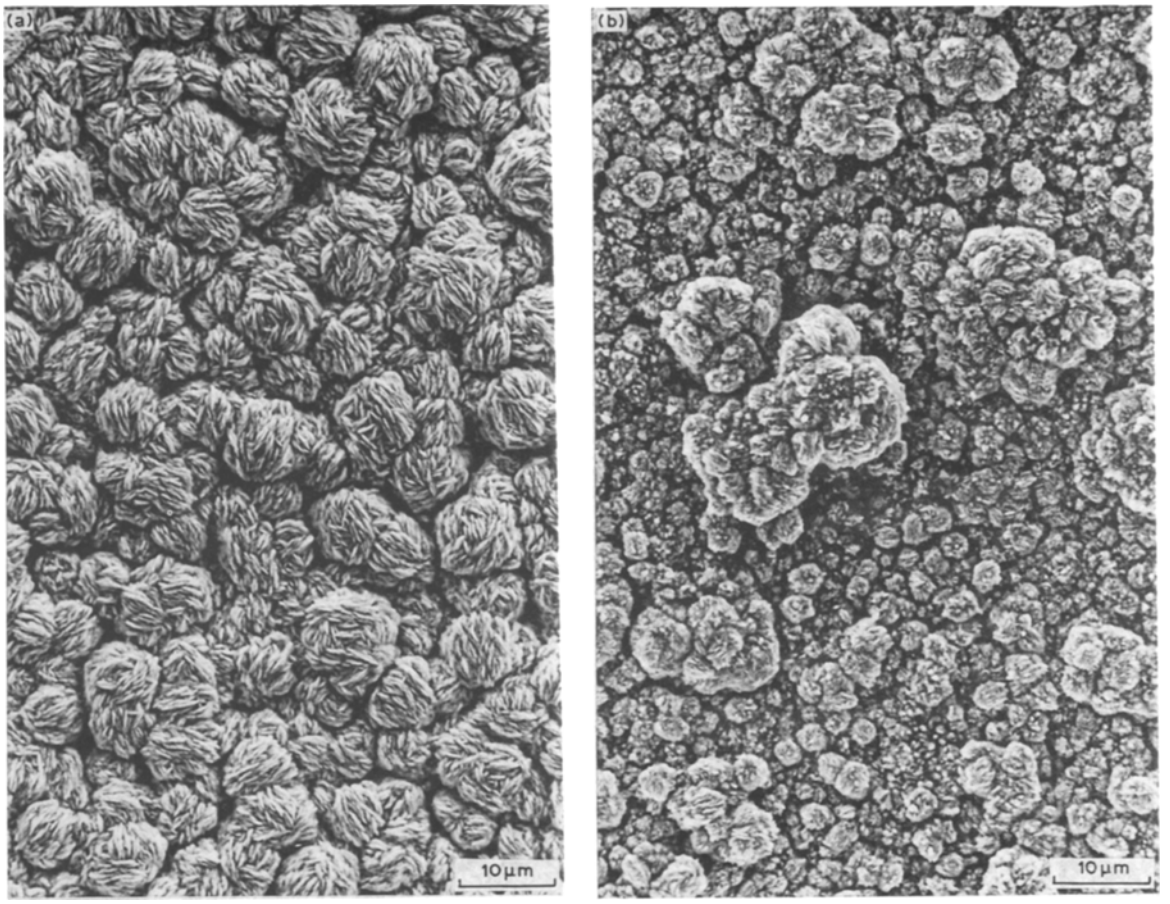

Fig. 8. Deposits obtained in the following conditions: $[ZnSO_4] = 0.01$ M; i/i_L near 0.20; nozzle diameter: 0.5 mm; fluid velocity: 9.1 m s^{-1}; deposit thckness: 4.0 μm. (a) In the absence of pulsed laser beam, and (b) with 2 W laser beam.

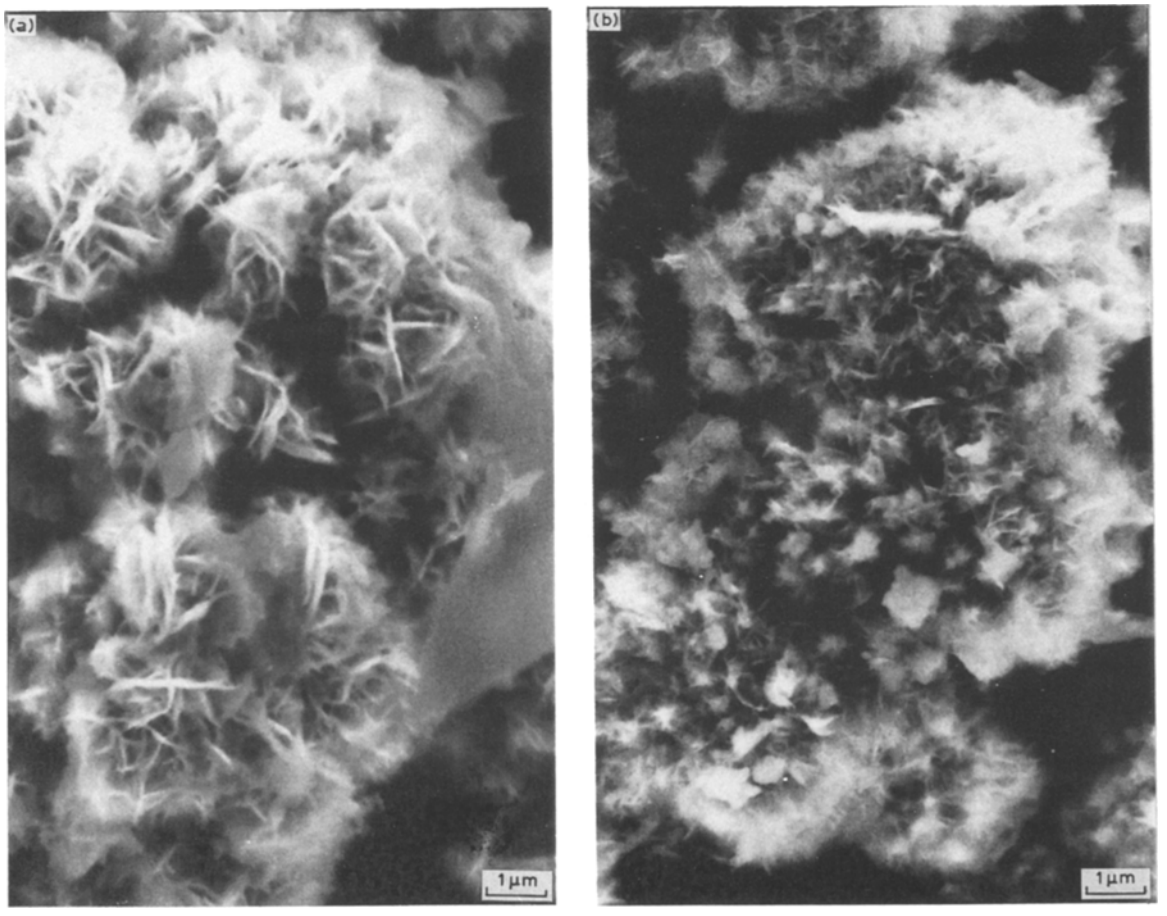

Fig. 9. Deposits obtained in the following conditions: $[ZnSO_4] = 0.01$ M; i/i_L near 0.87; nozzle diam.: 0.5 mm; fluid velocity: 9.1 m s^{-1}; deposit thickness: 3.4 μm. (a) In the absence of pulsed laser beam, and (b) with 2 W laser beam.

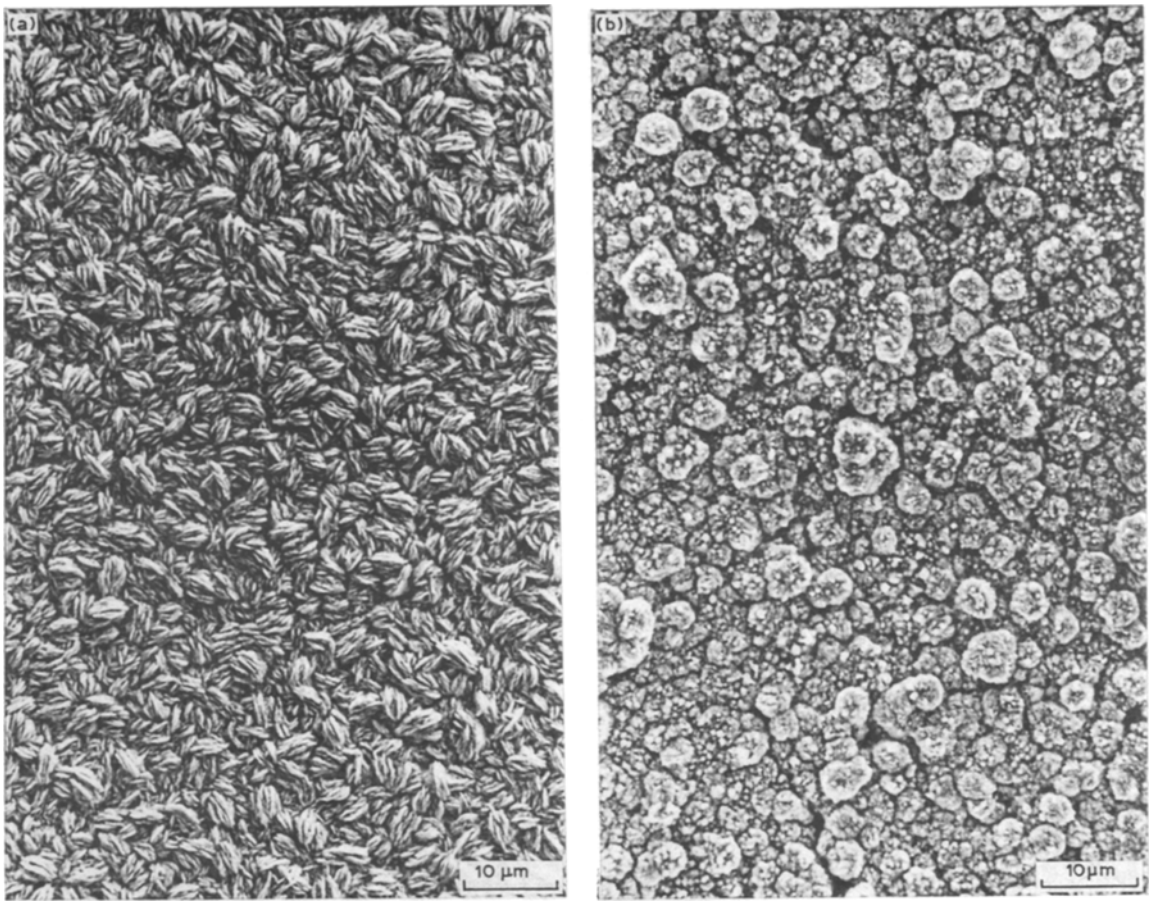

Fig. 10. Deposits obtained in the following conditions: $[ZnSO_4] = 0.07$ M; i/i_L near 0.03; nozzle diam.: 0.5 mm; fluid velocity: 9.1 m s^{-1}; deposit thickness: 3.7 μm. (a) In the absence of pulsed laser beam; and (b) with 2 W laser beam.

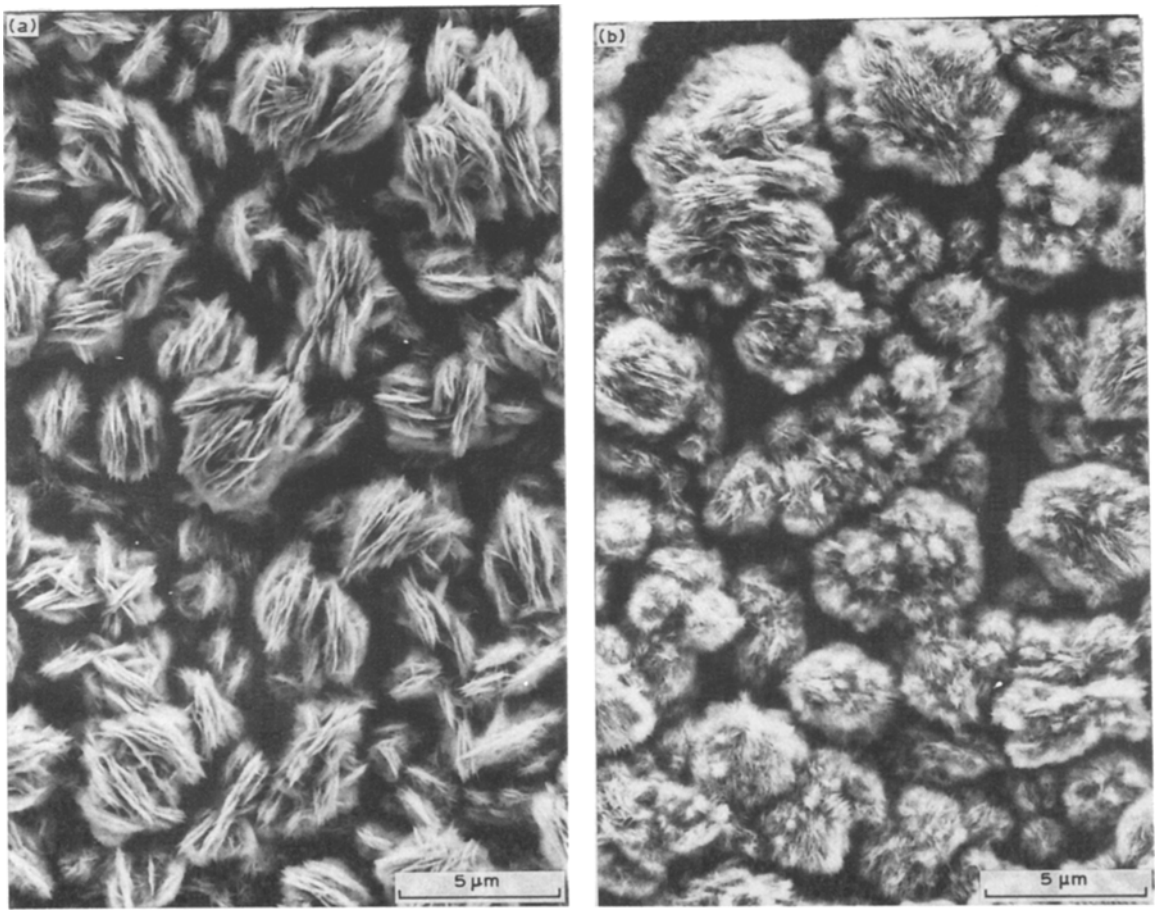

Fig. 11. Deposits obtained in the following conditions: $[ZnSO_4] = 0.07$ M; i/i_L near 0.12; nozzle diam.: 0.5 mm; fluid velocity: 9.1 m s^{-1}; deposit thickness: 3.4 μm. (a) In the absence of pulsed laser beam; and (b) with 2 W laser beam.

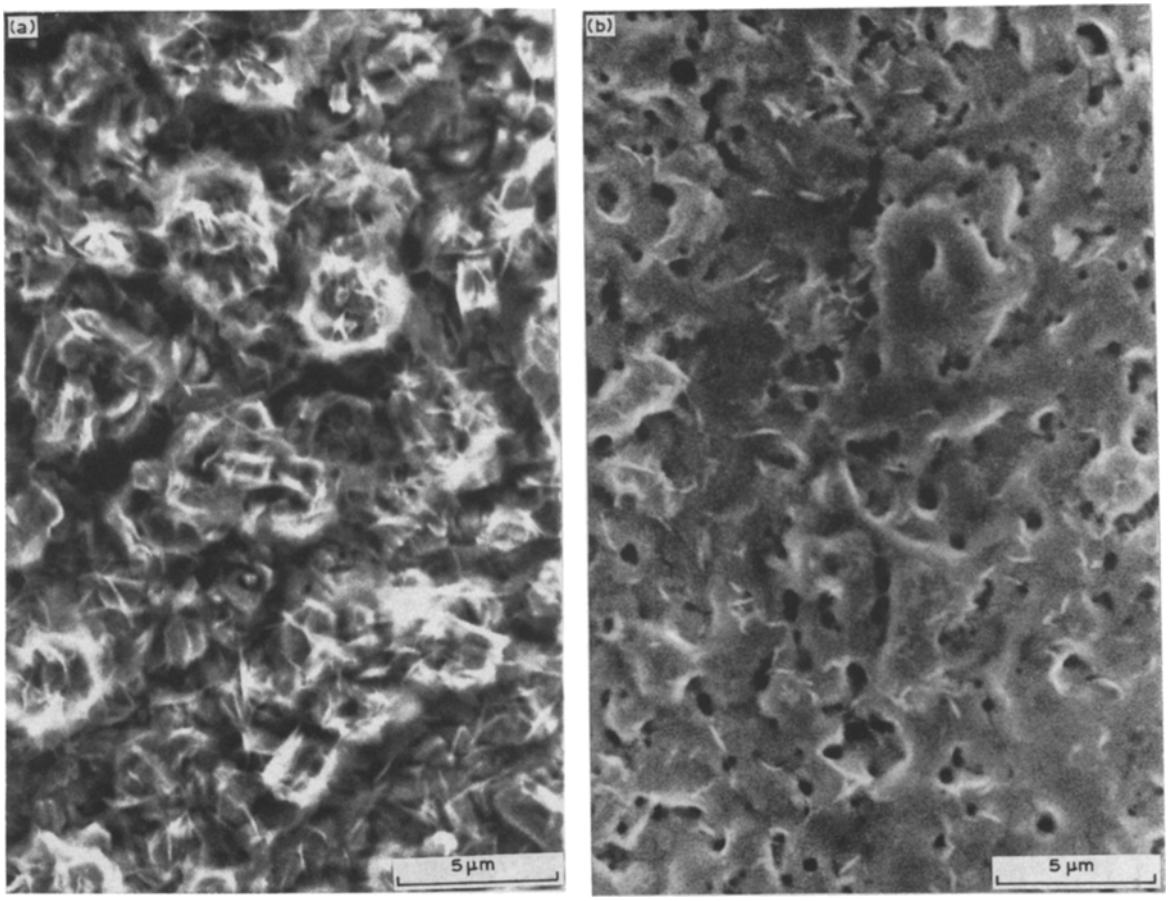

Fig. 12. Deposits obtained in the following conditions: $[ZnSO_4] = 0.7$ M; i/i_L near 0.004; nozzle diam.: 0.5 mm; fluid velocity: 9.1 m s^{-1}; deposit thickness: 5.4 μm. (a) In the absence of pulsed laser beam, and (b) with 2 W laser beam.

motionless conditions: the effect of the laser is thus less significant for processes with high deposition rates.

Acknowledgements

The authors are indebted to the Institut National Polytechnique de Lorraine (INPL, Nancy, France) for financial support, and to Dr. J. C. André of the Departement de Chimie Physique des Réactions, URA CNRS 328, for discussions and the use of the YAG laser source. Thanks are due to J. F. Rémy for assistance in scanning electron microscopy.

References

[1] D. T. Chin and R. R. Chandran, *J. Electrochem. Soc.* **125** (1978) 1461.
[2] R. G. Compton, A. C. Fisher and G. P. Tyley, *J. Appl. Electrochem.* **20** (1990) 912.
[3] R. G. Compton, C. R. Greaves and A. M. Waller, *ibid.* **20** (1990) 575.
[4] M. Datta, L. T. Romankiw, D. R. Vigliotti and R. J. von Gutfeld, *J. Electrochem. Soc.* **136** (1989) 2251.
[5] C. J. Raub, *Trans. Inst. Metal Finish.* **68** (1990) 115.
[6] R. J. von Gutfeld, *IEEE Circuits and Devices Magazine*, (Jan. 1986) 57.
[7] *Idem, J. Opt. Soc. Am. B,* **4** (1987) 272.
[8] J. C. Puippe, R. E. Acosta and R. J. von Gutfeld, *J. Electrochem. Soc.* **128** (1981) 2945.
[9] P. Bindra, G. V. Arbach and U. Stimming, *ibid.* **134** (1987) 2893.
[10] M. C. Hsiao and C. C. Wan, *ibid.* **138** (1991) 2273.
[11] I. Zouari, F. Lapicque, M. Calvo and M. Cabrera, *ibid.* **139** (1992) 2163.
[12] I. Zouari, M. Calvo, F. Lapicque and M. Cabrera, *Appl. Surf. Sci.* **54** (1992) 311.
[13] I. Zouari and F. Lapicque, *Electrochim. Acta* **37** (1992) 439.
[14] J. T. Davies, 'Turbulence Phenomena', Academic Press, New York (1972).
[15] D. T. Chin and K. L. Hsueh, *Electrochim. Acta,* **31** (1986) 561.
[16] A. Bensmaili and F. Coeuret, *J. Electrochem. Soc.* **137** (1990) 1744.
[17] D. T. Chin and C. H. Tsang, *ibid.* **125** (1978) 1461.